Baryon Spectroscopy with FLIC fermions

B. G. Lasscock, J. Hedditch, W. Kamleh, D. B. Leinweber, W. Melnitchouk, A. W. Thomas, A. G. Williams, R. D. Young, J. M. Zanotti

CSSM, University of Adelaide

July 31, 2006

Baryon Spectroscopy with FLIC Fermions

Aims of this presentation

- The nucleon resonances in QLQCD at light quark masses.
  - We review the spectrum of excited states of N and Δ.
  - Consideration is given to extracting the Roper resonance.
  - Reveal chiral curvature in the Δ^{++}.
- Search for the Θ^+ pentaquark in QLQCD.
  - We review the spectrum of our 5-quark interpolators.
  - We present the details of our analysis.
  - Comparison with Doi et al. and our lattice simulations.

Outline

Nucleon resonances

Search for the Θ^+ pentaquark

Form factors of spin-1 mesons, with FLIC fermions

Interpolating Fields

Nucleon interpolating fields,

$$\begin{aligned}\chi_1(x) &= \epsilon^{abc}(u^{Ta}(x)C\gamma_5 d^b(x))u^c(x)\\ \chi_2(x) &= \epsilon^{abc}(u^{Ta}(x)Cd^b(x))\gamma_5 u^c(x)\\ \chi_3^\mu(x) &= \epsilon^{abc}(u^{Ta}(x)C\gamma_5\gamma^\mu d^b(x))\gamma_5 u^c(x)\end{aligned}$$

Δ interpolating field,

$$\chi^\mu_{\Delta^{++}}(x) = \epsilon^{abc}(u^{Ta}(x)C\gamma^\mu u^b(x))u^c(x)$$

2pt Functions at the Hadronic Level

The correlation function, $\mathcal{G}$, of the interpolating field χ at time t and momentum $\vec{p}$ as

$$\mathcal{G}(t,\vec{p}) \;=\; \sum_{\vec{x}} \exp(-i\vec{p}\cdot\vec{x})\,\langle 0\,|\,T\;\chi(x)\;\bar{\chi}(0)\;|\,0\rangle$$

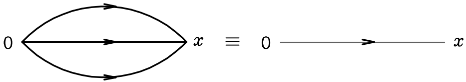

Inserting a complete set of momentum, energy and spin states, and using translational invariance,

$$\mathcal{G}(t,\vec{p}) = \sum_B e^{-E_B t} \times \sum_s \langle 0|\;\chi(0)\;|B,\vec{p},s\rangle\langle B,\vec{p},s|\;\bar{\chi}(0)\;|0\rangle$$

2pt Functions at the Hadronic Level

The correlation function, $\mathcal{G}$, of the interpolating field χ at time t and momentum $\vec{p}$ as

$$\mathcal{G}(t,\vec{p}) \;=\; \sum_{\vec{x}} \exp(-i\vec{p}\cdot\vec{x})\,\langle 0\,|\,T\;\chi(x)\;\bar{\chi}(0)\;|\,0\rangle$$

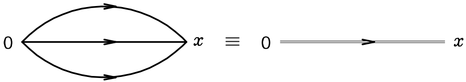

Inserting a complete set of momentum, energy and spin states, and using translational invariance,

$$\mathcal{G}^{\mu\nu}(t,\vec{p}) = \sum_{B} e^{-E_B t} \times \sum_{s} \langle 0|\;\chi^{\mu}(0)\;|B,\vec{p},s\rangle\langle B,\vec{p},s|\;\bar{\chi}^{\nu}(0)\;|0\rangle$$

Spin-1/2 Correlation Functions at the Hadronic Level

Following Melnitchouk et al., Phys. Rev. D67, 114506, 2003

Phenomenology of spin-1/2 states,

$$\langle \Omega \,|\, \chi_{1,2}(0) \,|\, B^+, \vec{p}, s \rangle = \lambda_{B^+} \sqrt{\frac{M_{B^+}}{E_{B^+}}}\, u_{B^+}(p,s)$$

$$\langle \Omega \,|\, \chi_{1,2}(0) \,|\, B^-, \vec{p}, s \rangle = \lambda_{B^-} \sqrt{\frac{M_{B^-}}{E_{B^-}}}\, \gamma_5 u_{B^-}(p,s)$$

$$\langle 0 | \chi^{\mu}_{3,\Delta} | N^{\frac{1}{2}^+}(p,s) \rangle = (\alpha_{1/2^+} p^{\mu} + \beta_{1/2^+} \gamma^{\mu}) \sqrt{\frac{M_{1/2^+}}{E_{1/2^+}}}\, \gamma_5 u(p,s)$$

$$\langle 0 | \chi^{\mu}_{3,\Delta} | N^{\frac{1}{2}^-}(p,s) \rangle = (\alpha_{1/2^-} p^{\mu} + \beta_{1/2^-} \gamma^{\mu}) \sqrt{\frac{M_{1/2^-}}{E_{1/2^-}}}\, u(p,s)$$

$$\sum_s u_B(p,s) \bar{u}_B(p,s) = \frac{(\gamma \cdot p + M_B)}{2M_B}$$

Spin-3/2 Correlation Functions at the Hadronic Level

Following Melnitchouk et al., Phys. Rev. D67, 114506, 2003
Phenomenology of spin-3/2 states,

$$\langle 0|\chi_\mu|N^{\frac{3}{2}+}(p,s)\rangle = \lambda_{3/2^+}\sqrt{\frac{M_{3/2^+}}{E_{3/2^+}}}\, u_\mu(p,s)$$

$$\langle 0|\chi_\mu|N^{\frac{3}{2}-}(p,s)\rangle = \lambda_{3/2^-}\sqrt{\frac{M_{3/2^-}}{E_{3/2^-}}}\, \gamma_5 u_\mu(p,s)$$

$$\sum_s u^\mu(p,s)\bar{u}^\nu(p,s) = \frac{(\gamma\cdot p+m)}{2m}\Big\{ g^{\mu\nu} - \frac{1}{3}\gamma^\mu\gamma^\nu - \frac{2p^\mu p^\nu}{3m^2} + \frac{p^\mu\gamma^\nu - p^\nu\gamma^\mu}{3m} \Big\}$$

Projection Operators

States of specific parity extracted with,

$$\Gamma^{\mp} = \frac{1}{2}\left(1 \pm \frac{M_{B^{\pm}}}{E_{B^{\pm}}}\gamma_0\right)$$

States of specific spin extracted with,

$$\begin{aligned} P^{\frac{3}{2}}_{\mu\nu}(p) &= g_{\mu\nu} - \frac{1}{3}\gamma_\mu\gamma_\nu - \frac{1}{3p^2}(\gamma \cdot p\gamma_\mu p_\nu + p_\mu\gamma_\nu\gamma \cdot p) \\ P^{\frac{1}{2}}_{\mu\nu}(p) &= g_{\mu\nu} - P^{\frac{3}{2}}_{\mu\nu}(p) \end{aligned}$$

Lattice simulation parameters

- Simulations done on a $20^3 \times 40$ lattice, $a = 0.128$ fm.
- 400 gauge field configurations.
- Smallest $m_\pi = 300$ MeV.
- Zanotti et al., Phys. Rev. D71, 034510, 2005
  We use the FLIC fermion action for improved scaling.

Summary of nucleon resonances

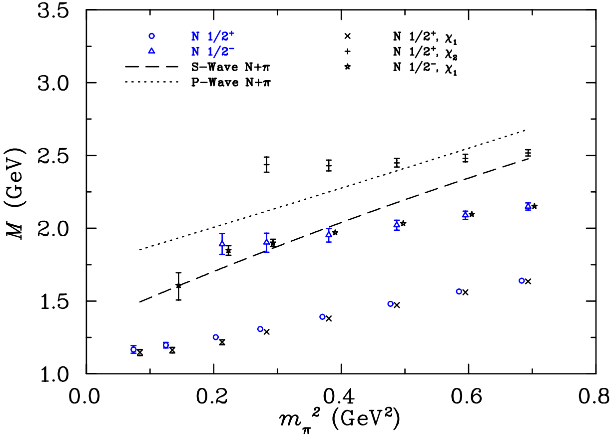

Summary of nucleon resonances

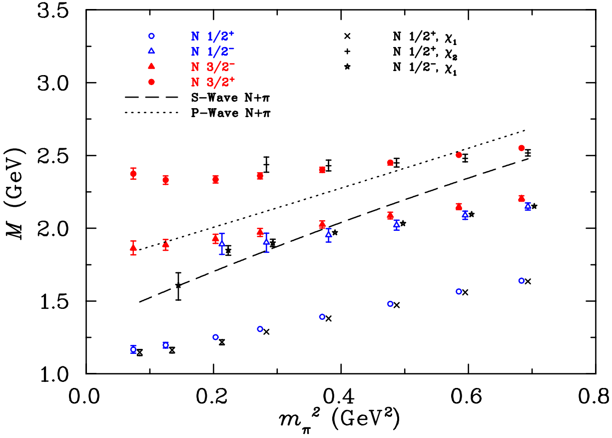

Summary of Δ resonances

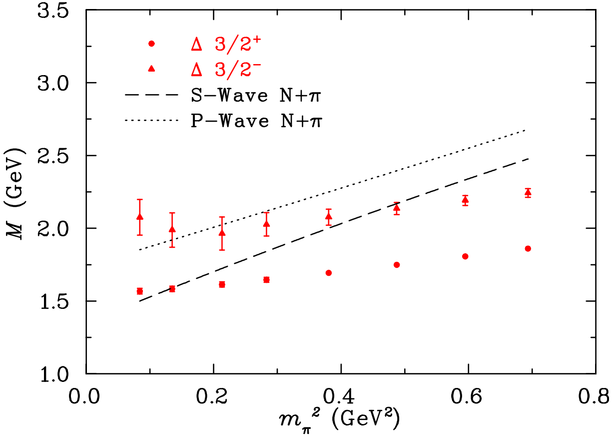

Summary of Δ resonances

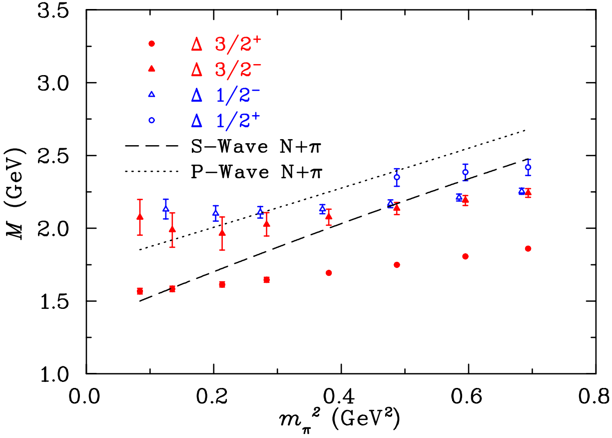

Summary of Δ resonances

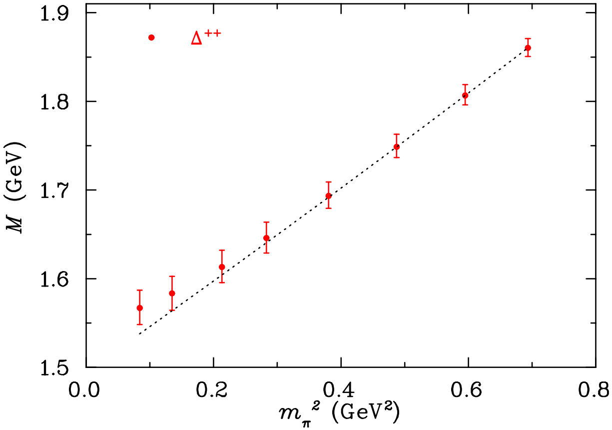

Our χ_1, χ_2, χ_3 Roper search

To construct the correlation matrix we evaluate the cross terms,

$$\mathcal{G}^{\mu}(t,\vec{p}) = \sum_B e^{-E_B t} \times \sum_s \langle 0|\chi_3^{\mu}(0)\ |B,\vec{p},s\rangle\langle B,\vec{p},s|\ \bar{\chi}_{1,2}(0)\ |0\rangle$$

$$\mathcal{G}^{\mu}(t,\vec{p}) = \sum_B e^{-E_B t} \times \sum_s \langle 0|\chi_{1,2}(0)\ |B,\vec{p},s\rangle\langle B,\vec{p},s|\ \bar{\chi}_3^{\mu}(0)\ |0\rangle$$

2×2 Correlation Matrix Analysis

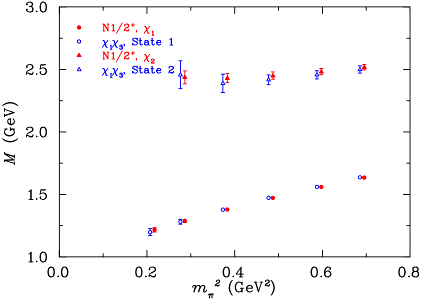

χ_1 and χ_3

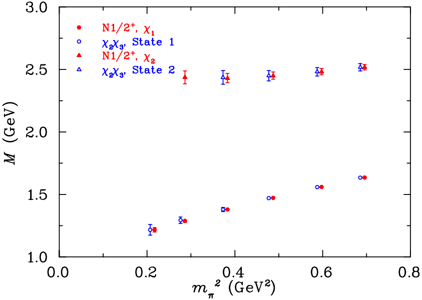

χ_2 and χ_3

Fierz transformation of χ_3

Results suggested that χ_3 has significant overlap with χ_1, χ_2. Using the Fierz identity,

$$\delta_{\alpha\alpha'}\delta_{\beta\beta'} = \frac{1}{4}\sum_J (\Gamma_J)_{\alpha\beta}(\Gamma_J^{-1})_{\beta'\alpha'}$$

$$\chi_3^\mu = -\frac{1}{4}\gamma^\mu\gamma_5\chi_{\rm Ioffe} - \frac{1}{8}\gamma^\mu\gamma_5\chi_{\rm A} + \frac{1}{2}\epsilon^{abc}(u^{aT}C\gamma^\mu u^b)d^c - \frac{i}{2}\epsilon^{abc}(u^{aT}C\sigma^{\mu\alpha}u^c)\gamma_\alpha d^c$$

D.B. Leinweber, Phys. Rev. D51, 6383-6393, 1995

$$\chi_{\rm Ioffe} = \epsilon^{abc}(u^{aT}C\gamma^\alpha u^b)\gamma_5\gamma_\alpha d^c$$
$$\chi_{\rm A} = \epsilon^{abc}(u^{aT}C\sigma^{\alpha\beta}u^b)\gamma_5\sigma_{\alpha\beta}d^c$$

3×3 Correlation Matrix Analysis

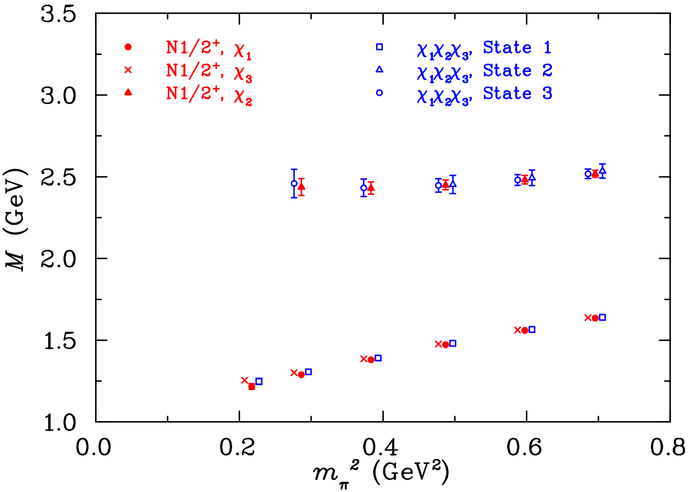

Summary

- Nucleon spectrum successfully simulated a light quark masses.
- Effects of the open decay channel important can be important.
- Chiral curvature observed in the Δ^{++}
- We do not extract a state consistent with the Roper.

Outline

Nucleon resonances

Search for the Θ^+ pentaquark

Form factors of spin-1 mesons, with FLIC fermions

NK-type Interpolating Field

- Csikor *et al*, JHEP 0311:070,(2003)
- Spin-1/2, isospin 0,1

$$
\begin{aligned}
\chi_{NK} &= \frac{1}{\sqrt{2}}\epsilon^{abc}(u^{Ta}C\gamma_5 d^b)\left\{u^c(\bar{s}^e i\gamma_5 d^e) \mp (u \leftrightarrow d)\right\} \\
\chi_{\widetilde{NK}} &= \frac{1}{\sqrt{2}}\epsilon^{abc}(u^{Ta}C\gamma_5 d^b)\left\{u^e(\bar{s}^e i\gamma_5 d^c) \mp (u \leftrightarrow d)\right\}
\end{aligned}
$$

The $\mp$ for isospin $I = 0$ and 1 channels, respectively.

Diquark-Diquark Style Interpolating Fields

- Sasaki Phys. Rev. Lett. **93** 152001 (2004).
- Spin-1/2, isospin 0

$$\chi_{PS} = \epsilon^{abc}\epsilon^{aef}\epsilon^{bgh}(u^{eT}Cd^f)(u^{gT}C\gamma_5 d^h)C\bar{s}^{cT}$$

- Our SS-type interpolating field, Phys.Rev.**D72** 014502,(2005).
- Spin-1/2, isospin 1

$$\chi_{SS} = \frac{1}{\sqrt{2}}\epsilon^{abc}(u^{Ta}C\gamma_5 d^b)(u^{Tc}C\gamma_5 d^e)C\bar{s}^{Te}$$

Results, $I(J^P) = 0(1/2^-)$

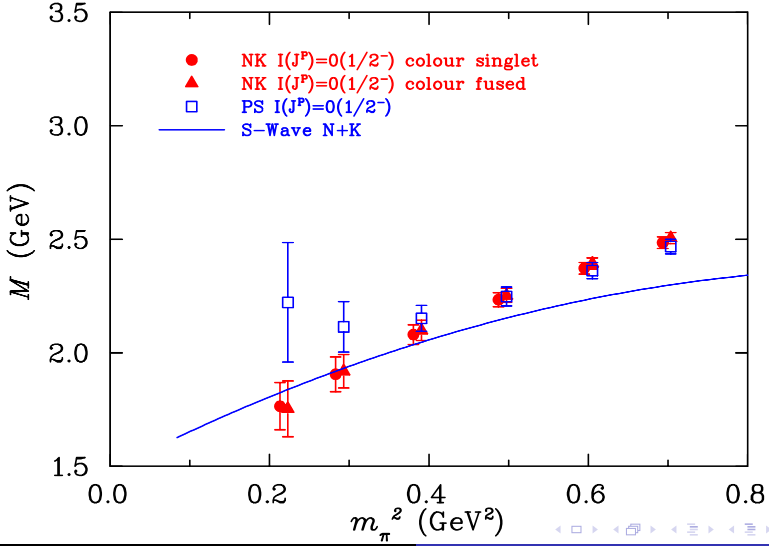

Mass Splitting, $I(J^P) = 0(1/2^-)$

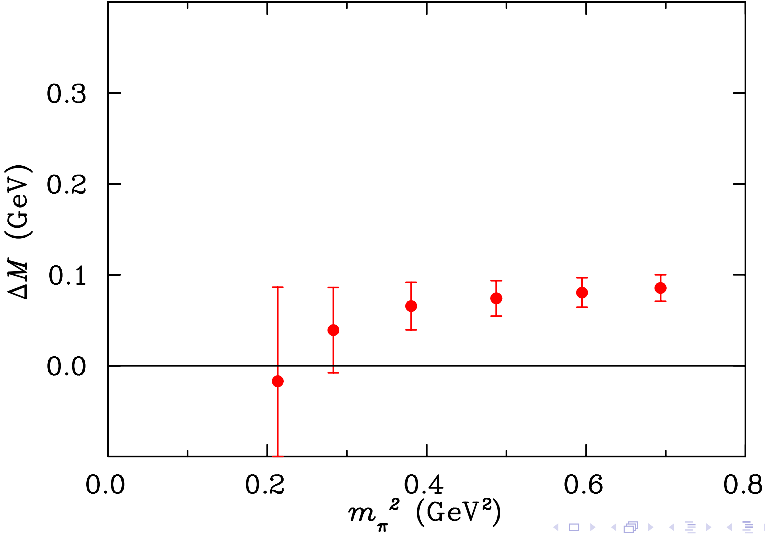

Results, $I(J^P) = 1(1/2^-)$

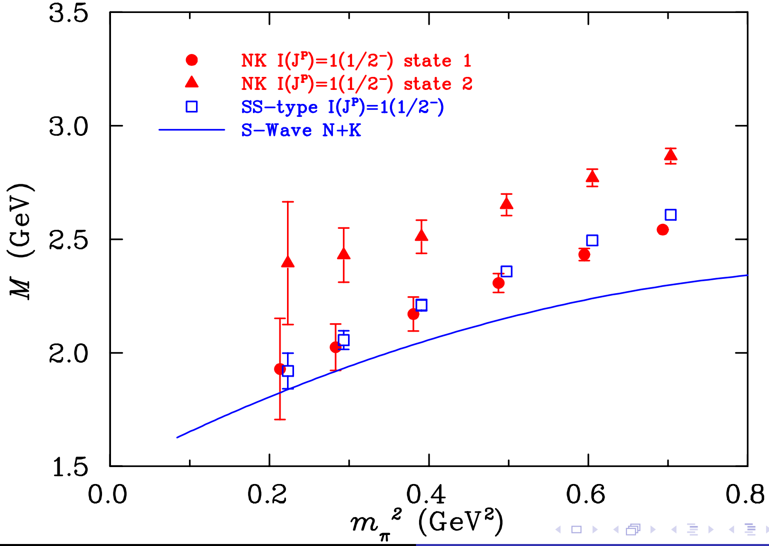

Summary, $I(J^P) = 0(1/2^-)$

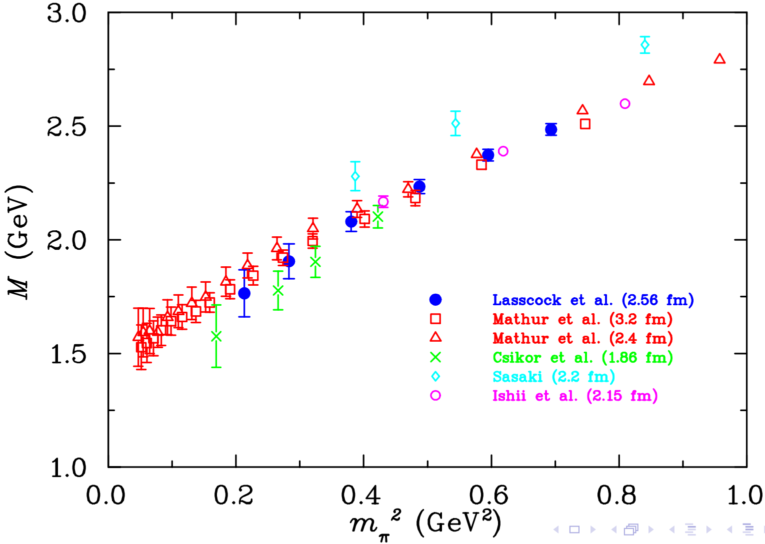

Results, $I(J^P) = 0, 1(1/2^+)$

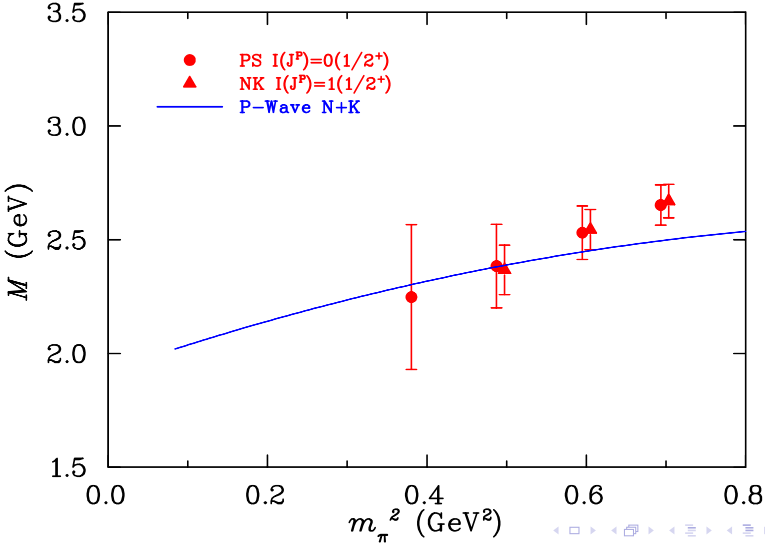

Mass Splitting, $I(J^P) = 0(1/2^+)$

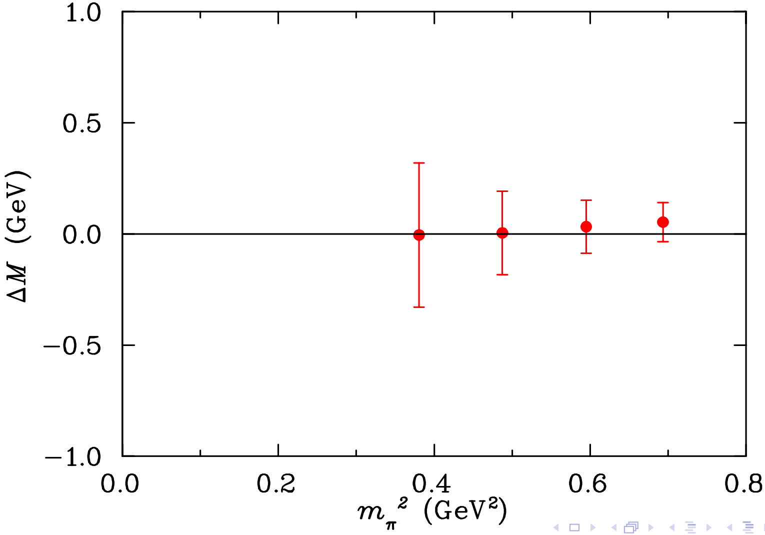

Spin-3/2 Pentaquark Interpolating Field

- **Lasscock et al., Phys D72, 074507, 2005**
- Couples to both Spin-1/2 and Spin-3/2 states, isospin 0,1

$$\chi^{\mu}_{NK^*} = \frac{1}{\sqrt{2}}\epsilon^{abc}(u^{Ta}C\gamma_5 d^b)\{u^c(\bar{s}^e i\gamma^\mu d^e) \mp (u \leftrightarrow d)\} \ ,$$

$$\chi^{\mu}_{LY} = \epsilon^{abc}(u^{Ta}C\gamma_5\gamma^\mu d^b)\Big\{ (u^{Tc}C\gamma_5 d^e) \mp (u^{Te}C\gamma_5 d^c)\Big\} C\bar{s}^{eT}$$

The $\mp$ for isospin $I = 0$ and 1 channels, respectively.

- Phenomenology and projection operators based on nucleon resonance study.

Error Bars

Efron, An Introduction to the Bootstrap

The jackknife sample of the mean is calculated with one of the data points excluded,

$$\bar{x}_i = \frac{1}{n-1} \sum_{j \neq i}^{n} x_j \tag{1}$$

The usual estimate of the variance is then,

$$\sigma^2 = \frac{n-1}{n} \sum_{i}^{n} (\bar{x}_i - \frac{1}{n} \sum_{j}^{n} \bar{x}_j)^2 \tag{2}$$

Jackknife Subensembles

Efron, An Introduction to the Bootstrap

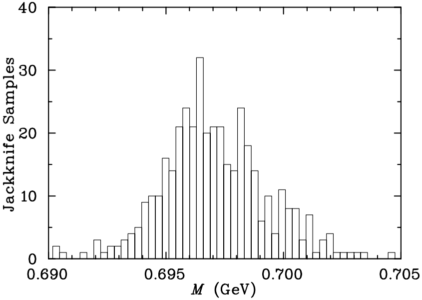

Pion

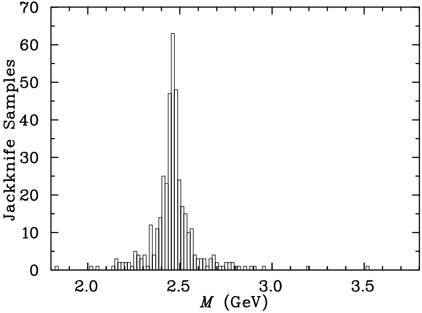

$0(3/2^+)$ pentaquark

Jackknife Subensembles

Efron, An Introduction to the Bootstrap

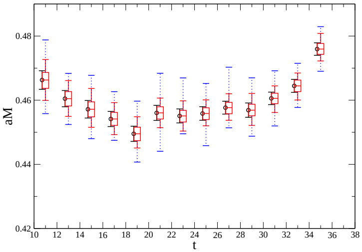

Pion

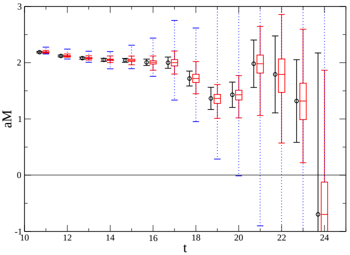

$0(3/2^+)$ pentaquark

Isoscalar odd parity states

Effective mass of the $I(J^P) = 0(3/2^-)$ state extracted with the LY interpolator.

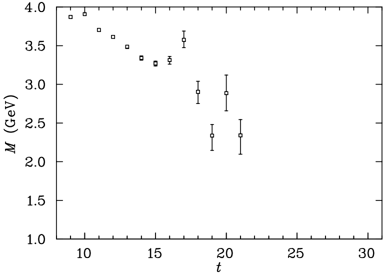

Isoscalar odd parity states

χ^2_{dof} at the largest quark mass.

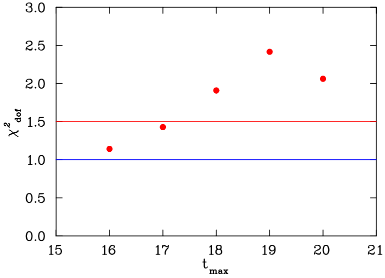

Lower bound fixed at t=14

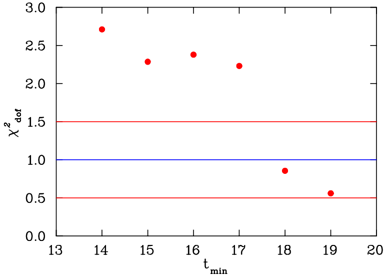

Upper bound fixed at t=21

Isoscalar odd parity states

Effective mass of the $I(J^P) = 0(3/2^-)$ state extracted with the LY interpolator.

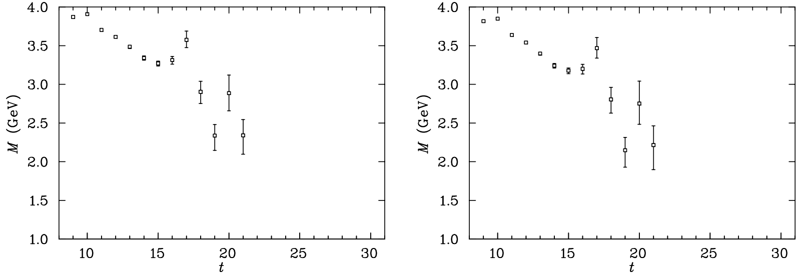

Isoscalar odd parity states

χ^2_{dof} at the largest quark mass.

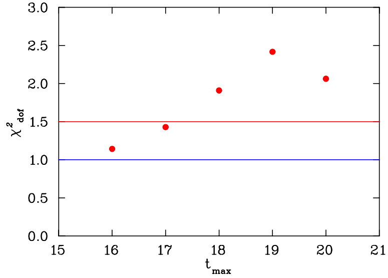

Lower bound fixed at t=14

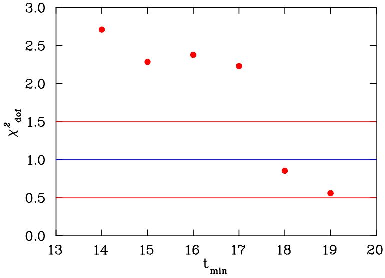

Upper bound fixed at t=21

Isoscalar odd parity states

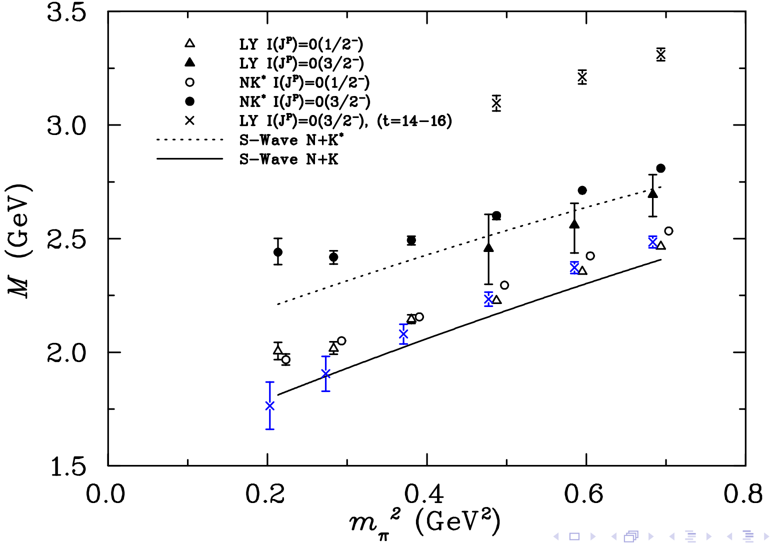

Isoscalar even parity states

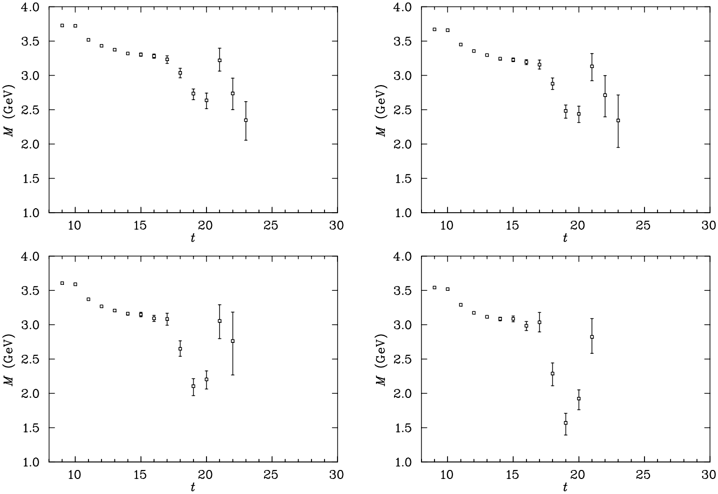

Isoscalar even parity states

$\chi^2_{\rm dof}$ at the third largest quark mass.

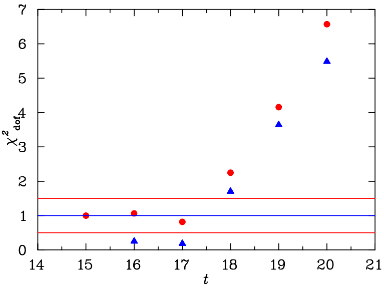

Lower bound at t=12 and t=13

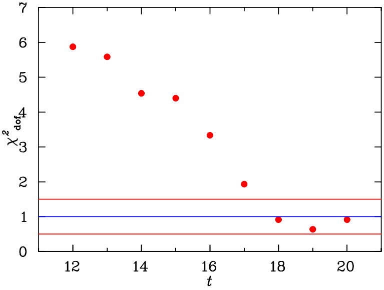

Upper bound fixed at t=22

Isoscalar even parity states

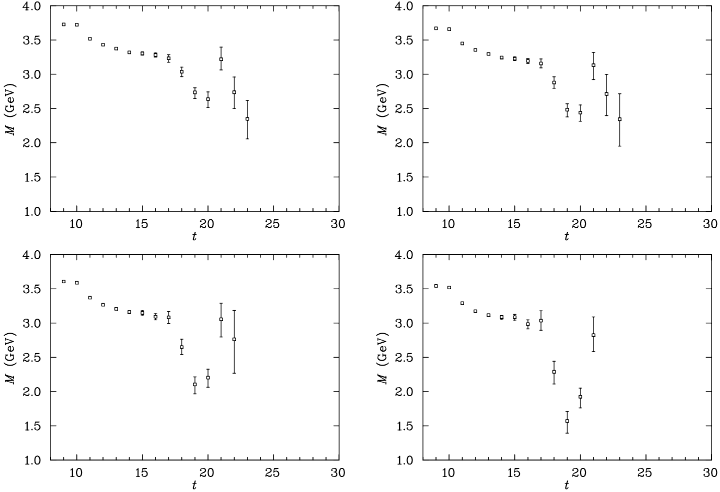

Isoscalar even parity states

$\chi^2_{\rm dof}$ at the third largest quark mass.

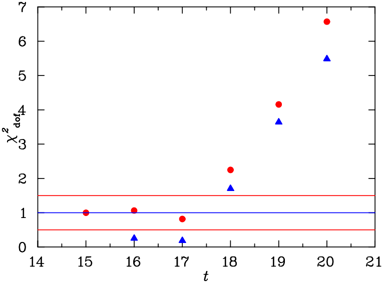

Lower bound at t=12 and t=13

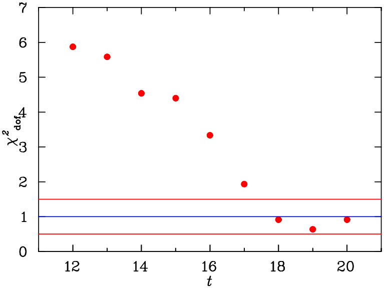

Upper bound fixed at t=22

Isoscalar even parity states

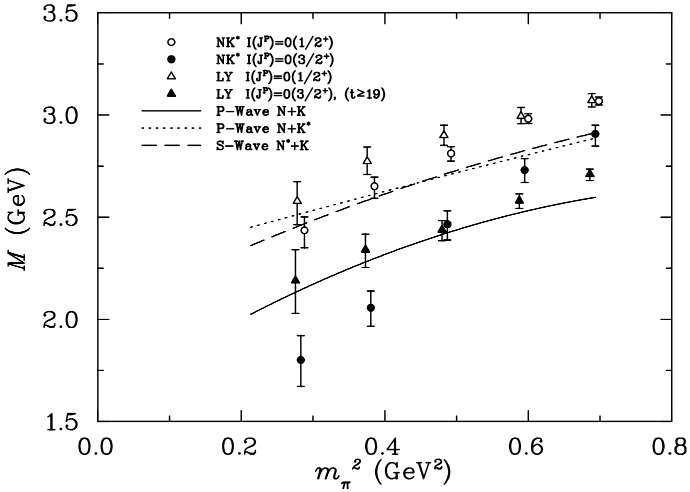

Isoscalar even parity states

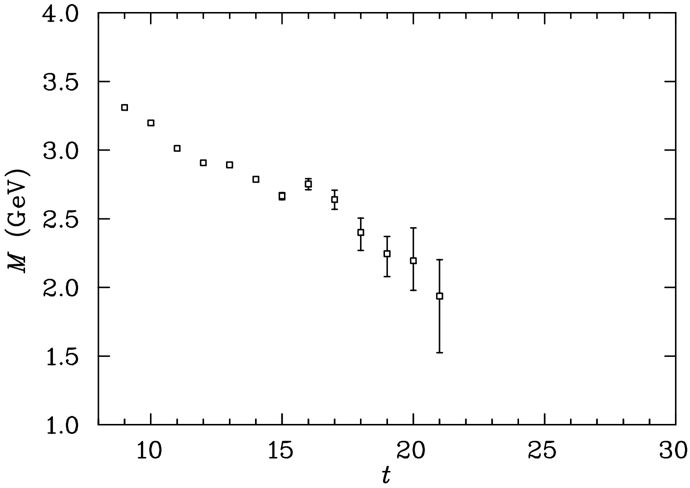

Summary of Spin-3/2 pentaquark calculations

Comparison with Phys. Rev. D72, 074503 (2005)

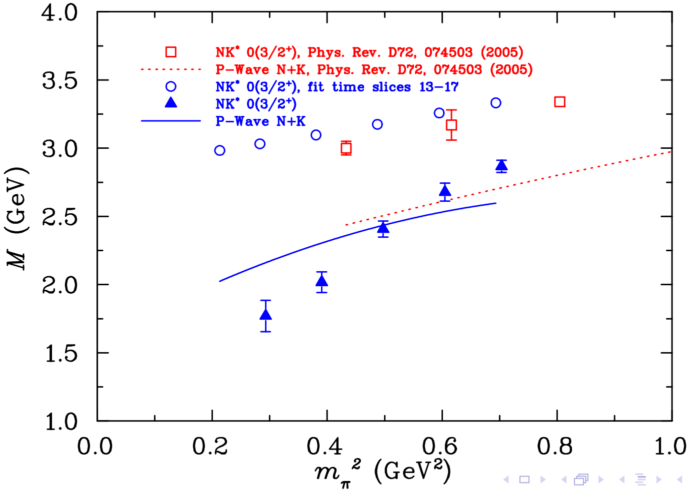

Summary of Spin-3/2 pentaquark calculations

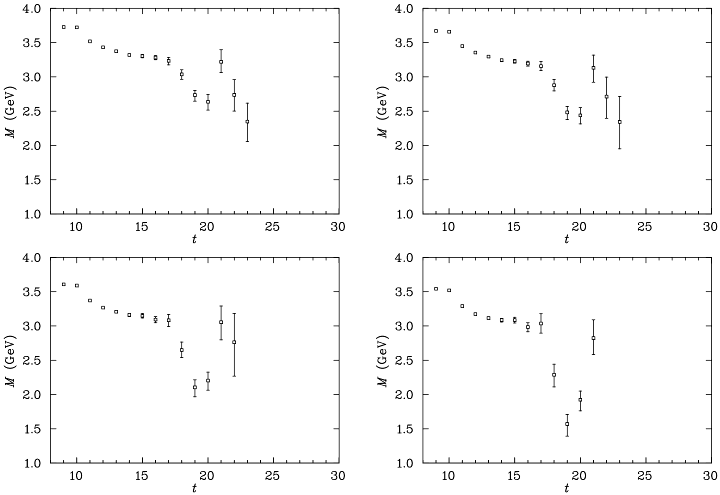

Summary of Spin-3/2 pentaquark calculations

$\chi^2_{\rm dof}$ at the third largest quark mass.

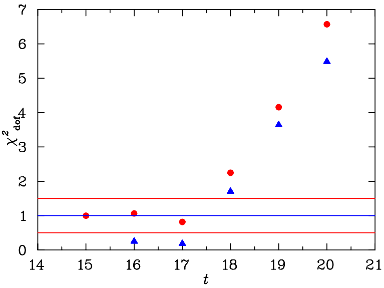

Lower bound at t=12 and t=13

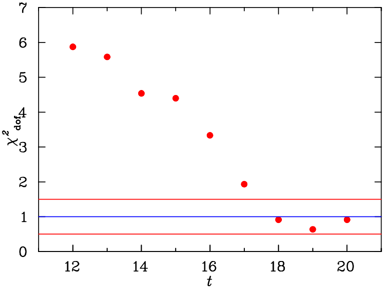

Upper bound fixed at t=22

Summary of Spin-3/2 pentaquark calculations

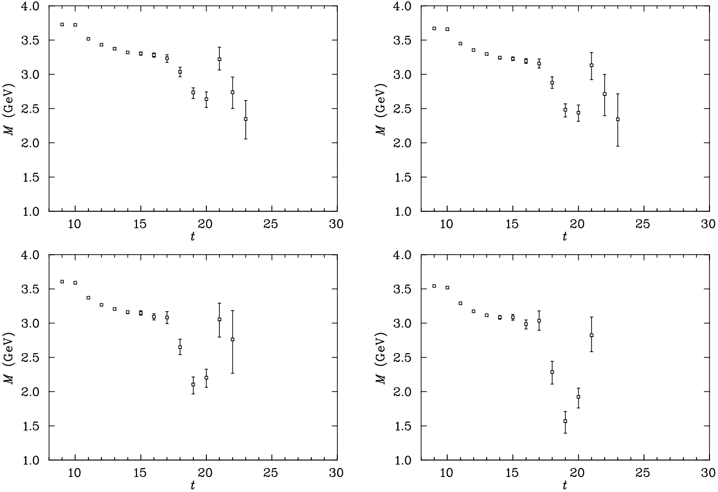

Summary of Spin-3/2 pentaquark calculations

Comparison with Phys. Rev. D72, 074503 (2005)

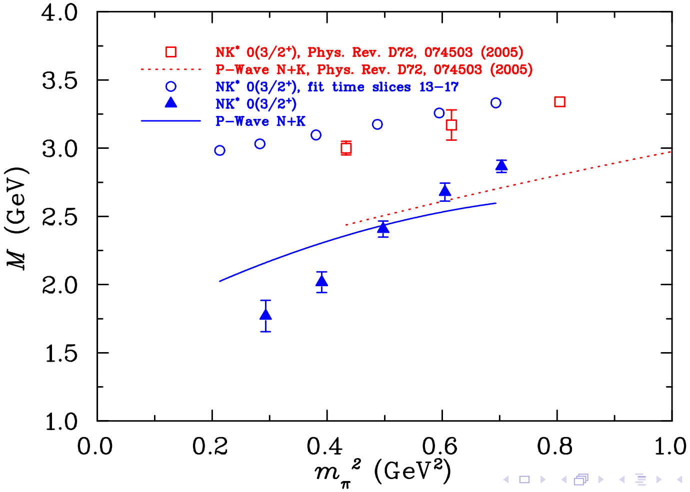

Summary of Spin-3/2 pentaquark calculations

Comparison with Phys. Rev. D72, 074503 (2005)

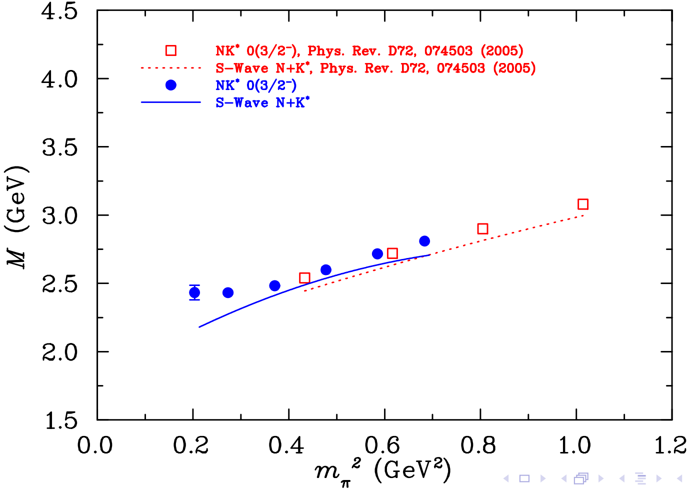

Summary

- No clear evidence of attraction is found in the spin-1/2 channel.
- "Sort and Cut" estimate of the confidence interval is more robust for the analysis of noisy pentaquark data.
- The size of the error bar does not determine the goodness of the fit.
- The discrepancy between our calculation and Doi et al. is due to the fit window.
- Evidence of attraction is found in the even parity, spin-3/2 Isoscalar, channel.

Outline

Electromagnetic Structure in Quenched LQCD

- Charge, magnetic and quadrapole form factors calculated in Quenched LQCD.
- Charge radii and magnetic moment derived.

- Quark Models:
  - Hyperfine interaction $\frac{(\sigma_1 \cdot \sigma_2)}{(m_1 m_2)}$.
  - Magnetic moment of the ρ meson, $\mu_\rho \simeq 1.84\mu_N$ at SU(3) flavour limit.

- Lattice QCD: Oblate ρ-meson?
  Alexandrou et al. Phys. Rev. D66, 094503, 2002

- Environmental sensitivity of observables?

Form Factors, Formulas

Following,

Brodsky and Hiller, Phys. Rev. D46, 2141–2149, 1992.

For the pion and kaon,

$$\langle p's'|J^\alpha|p,s\rangle = \frac{1}{2\sqrt{E_p E_{p'}}}\left[p^\alpha + p'^\alpha\right]F_1(Q^2)\ .$$

For the ρ and K^*,

$$\langle p's'|J^\mu|ps\rangle = \frac{1}{2\sqrt{E_p E_{p'}}}\,\epsilon'^\star_\alpha(p',s')\epsilon_\beta(p,s)J^{\alpha\mu\beta}(p',p)\ ,$$

$$J^{\alpha\mu\beta}(p',p) = -\{G_1(Q^2)\,g^{\alpha\beta}\left[p^\mu + p'^\mu\right] + G_2(Q^2)[g^{\mu\beta}q^\alpha - g^{\mu\alpha}q^\beta] - G_3(Q^2)\,q^\beta q^\alpha\,\frac{p^\mu + p'^\mu}{2M^2}\}\ .$$

Quark Sector Contributions to the Charge Radii

Quark Sector Contributions to the Charge radii $< r^2 >$ (fm^2).

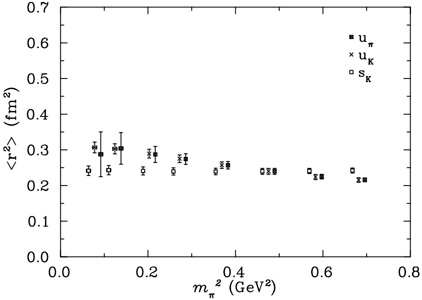

Pseudoscalar mesons

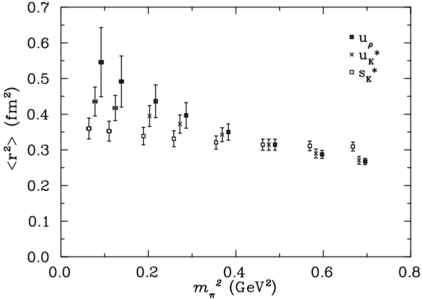

Vector mesons

Environmental Sensitivity of Charge Radii

Ratio of the up-quark contributions to $< r^2 >$ fm^2.

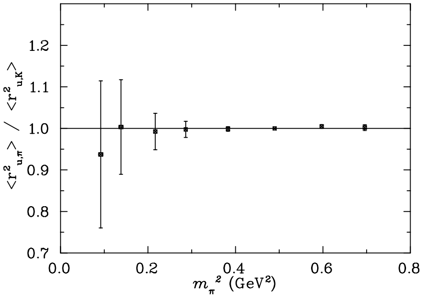

Pseudoscalar mesons

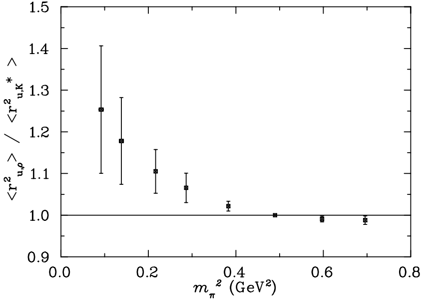

Vector mesons

Summary of the meson and proton charge radii

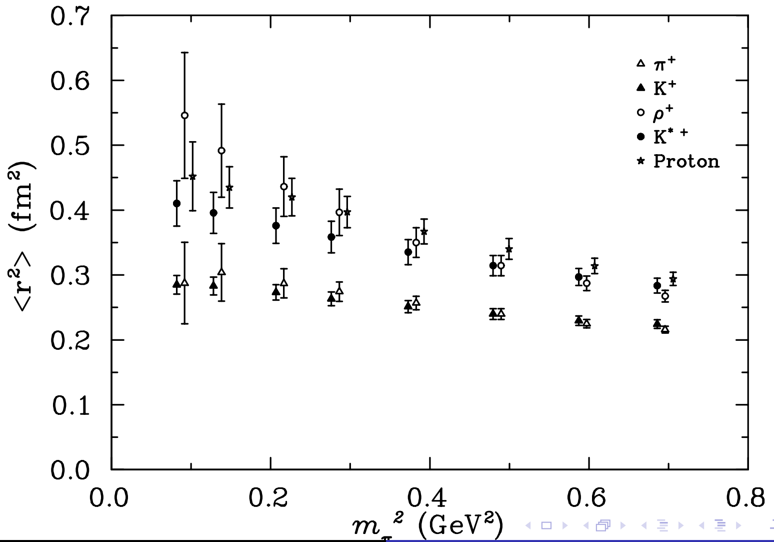

The Magnetic Moment

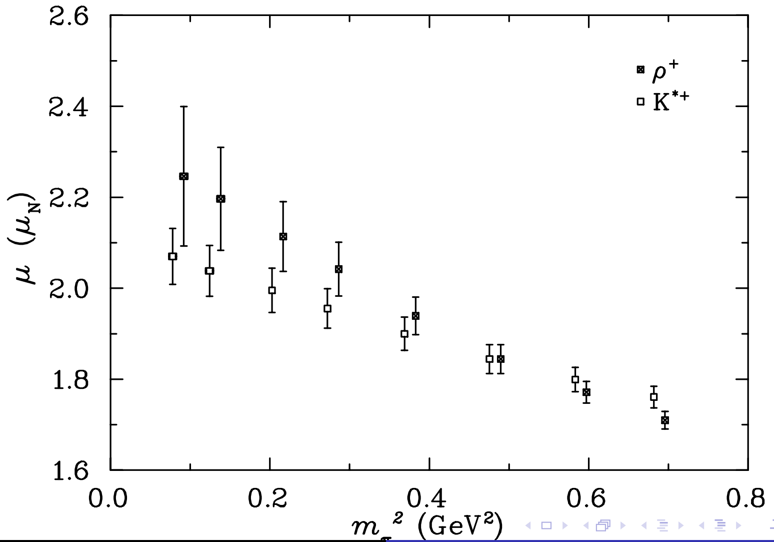

ρ-meson Quadrapole Form Factor

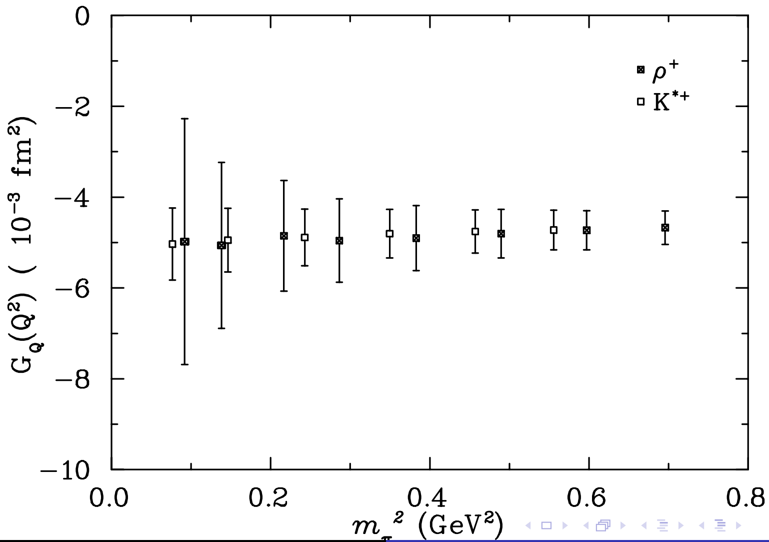

Summary

- Hyperfine repulsion in vector mesons on Quenched LQCD is significant.
- There is significant environmental sensitivity in the up quark contributions to vector meson charge radii.
- The charge radius of the proton is similar to that of the ρ-meson, but consistently larger than that of the pion and kaon.
- Vector mesons are oblate.

Criticism, Phys. Rev. D72, 074503 (2005)

There are a number of differences in the lattice QCD setup between the current studies and Ref. [67], such as the gauge and the quark actions, and the implementation of the smeared source. However, we consider that, rather than being a consequence of these differences, the discrepancy mainly comes from the low statistics adopted in Ref. [67]. We emphasize again that spin-3/2 pentaquark correlators are quite noisy, and therefore require better statistics.